

## Dynamics of Free Liquid Jets Affected by Obstructions at the Jet Entrance

V. N. Lad<sup>1</sup> and Z. V. P. Murthy<sup>1,2</sup>

**Abstract:** Free liquid jets are of great technical importance in a variety of applications like ink-jet printing, glass painting, spray coating and metal cutting. Here we consider the changes induced in the dynamics of such jets by the presence of obstructions at the tube exit. Using stainless steel bars of 1.5 mm diameter as obstruction objects and aqueous solutions of glycerol of varying concentrations as working fluids, we performed experiments for different configurations, including a single rod at the centre of the tube exit, two parallel rods equidistant from the centre of the tube, and a 10 mesh screen. Images of the jets coming through such restricted section were captured by high speed camera from two locations. We could observe a morphological change in the cross section of the liquid jet only for jets passing through a tube exit containing only one rod. The maximum expansion ratio of the jet decreased with the concentration of glycerol. Attempts were also made to correlate the characteristic jet diameter ratio with the Weber number. The findings discussed in the present work may provide a new direction for the design of new instruments for the measurement of surface tension or viscosity of liquids.

**Keywords:** Deformation of free liquid jet; perturbation; polymer additive; surface instability; surface tension measurement; surfactant.

### 1 Introduction

Free liquid jets are of great technical importance in a variety of applications like ink-jet printing, glass painting, spray coating, metal cutting, etc. Many studies have been done by various research groups to study the breakup of confined jets, free liquid jets, splashing of drops, bouncing droplets, spreading, cusps formation, etc. Kanemura, Yoshihashi-Suzuki, Kondo, Sugiura, Yamaoka, Ida, Nakamura, Matsushita, Muroga, and Horiike (2011) have studied the characteristics of free-surface

<sup>1</sup> Chemical Engineering Department, Sardar Vallabhbhai National Institute of Technology (NIT - Surat), Surat – 395007, Gujarat, India.

<sup>2</sup> Corresponding author. Tel.: +91 261 2201648 Fax: +91 261 2227334 E-mail: zvpm@ched.svnit.ac.in, zvpm2000@yahoo.com

waves on the high-speed liquid lithium jets. Begenir, Tafreshi, and Pourdeyhimi (2004) have found that cone-up nozzle produced water jets with shorter intact lengths, and cone-down or cylindrical nozzles produce constricted jets. Hiroyasu (2000) found that the cavitation at the nozzle-entrance decreased the breakup length. Wu, Miranda, and Faeth (1995) demonstrated that the length to diameter ratio of the constant cross section area of the nozzle passage also affects the onset of breakup of liquid jets along with the Reynolds number. Lee, Aalburg, Diez, Faeth, and Sallam (2007) have studied the breakup of turbulent round liquid jets in uniform crossflows and found that the formation of ligaments and droplets enhanced by the presence of crossflow. They concluded that the breakup times and distances of the turbulent columnar jets were smaller than that for non-turbulent liquid jets. Effects of obstructions in the liquid flow have been investigated by various researchers to find the pressure losses. Besides these attempts by various research groups, still the deformation characteristics of the jets flowing through the obstruction at the nozzle exit are not well understood. Hence, the fundamentals studies to know the effects of deformation of jets, and breakup length of jets due to obstructions at the nozzle exit are still needed. The present work is aimed to explore the consequences of obstructions at the nozzle exit on the breakup length of liquid jets.

## 2 Experimental Methods

Aqueous solutions of glycerol of varying concentrations were chosen as working fluids along with pure water and glycerol to investigate the dynamics of the jets. Sodium lauryl sulfate (Finar Chemicals, India) and Polyethylene oxide (National Chemicals, India) were used as additives as per requirement. Jets were prepared using the tubes of 4.6 mm, 6.1 mm and 9.2 mm diameters. The images of the jets were captured with the help of high speed motion camera X-PRI (AOS Technologies, Switzerland) capable of capturing images at 1000 frames per second. The dynamics of jets were studied by analyzing the captured images using the image analysis software.

Jets were produced at a velocity range from 0.4 m/s to 1.4 m/s at the tube exit. Experiments to study the deformation of free jet were repeated twice to confirm the reproducibility. The high speed camera was attached to a computer for camera control, and the frames were analyzed using the software Image J of NIH, USA to study the deformation/contraction and expansion of the jets. Figure 1 shows the schematic representation of experimental set up.

Any irregularity at the tip of the tube was removed with careful finishing the tube-end to make the exit end of tube almost completely flat. The length of the straight portion of the tube (without any bends or fittings measured from exit end of the tube) was more than at least 50 times its internal diameter so as to nullify the ef-

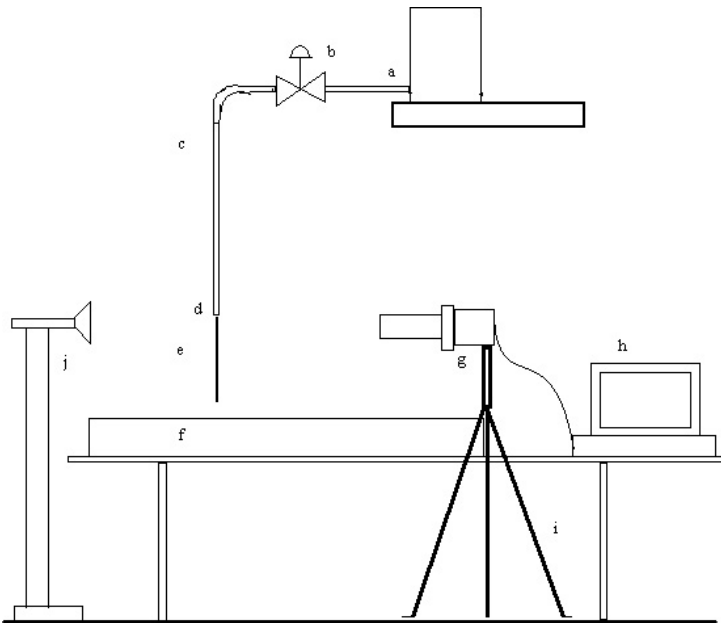


Figure 1: Schematic diagram of experimental set up: (a) reservoir, (b) control valve, (c) tube, (d) jet entrance (e) jet, (f) collection pan, (g) high speed camera, (h) computer, (i) tripod for camera, (j) illumination system

fects of entry length or any disturbances at the tube exit [Bird, Stewart, and Lightfoot (2002)]. Further, to minimize vibrations, the assembly of the tube was rigidly supported and the experimental set up was placed on a table compressing rubber gaskets between its legs and flooring.

Liquid solutions of aqueous glycerol of 10, 20, 30, 40 and 50% by mass were prepared by mixing glycerol with distilled water. Densities of all the solutions were calculated by taking known volumes of solutions and measuring their mass using Sartorius make weighing balance of 0.0001g resolution. Densities of the solutions were also checked from the literature for their accuracy and found error of less than 0.8%. Velocities of the fluid jet at jet entrance (tube-exit) were calculated by measuring volume of the fluid coming from the jet entrance, time of collecting that much amount of fluid, and cross-sectional area of the opening at the jet entrance. Surface tension and viscosity of the liquid solutions were taken from literature. A tank of 30 cm diameter and 40 cm height was used as reservoir for supplying glycerol-water solution. Liquid was supplied from the reservoir by means of gravity in certain experimental runs during which the level in the tank was kept almost constant during that particular experimental run by providing constant overflow. In some of the experimental runs, liquid was drawn through locally available

submersible pump which was able to develop 2.75 m liquid head. Prior to each experimental run, the tube was cleaned using the respective solutions of glycerol to avoid any contamination during initial period of the fluid passage through the tube. Extra precautions were taken to have proper illumination for high speed imaging by adjustment of illumination system, the diffuser screen and a shield to prevent direct light on the body of camera. The minimum limit of velocity was restricted by appearance of clear liquid jet after the initial dripping to jetting transition. The maximum limit of the velocity was limited to have jets which produce no excessive surface instability due to higher eddy formation inside the tube so as to have continuous columnar jet at the exit of the tube.

Solid rods of 1.5 mm diameter were used to provide obstruction at the jet exit. The straight cylindrical rods/hard wires of stainless steel were cut into pieces so as to fix it closely in the tip of the tube without making any change to the circular opening of the tube. To prevent any leakage of the liquid from the end joints of the rod, the ends of the rods were made curved by rubbing it carefully on the fine grinder wheel, to enable it to fix accurately with the inside surface of the tube. The ends of the solid rod were joined to the internal surface of the tube by means of adhesive and the assemblies were allowed at rest for at least 30 min to attain sufficient strength to the fixture prepared at tube exit. A piece of stainless steel screen of 10 mesh was cut circular and attached at the exit end of the plastic tube by means of suitable adhesive as shown in Fig. 2. Images of jets were captured from various locations as shown in Fig. 3. As at very low velocity the jet shows curvature and contracts diametrically, we measured the maximum diameter sufficiently downstream from the tube exit for better characterization and compensate initial disturbances.

### 3 Results and Discussion

Presence of the straight cylindrical obstruction at the entrance of the jet results in bifurcation of the jet at very high velocity and the jet breakup length does not have any significance in that case. Obstruction geometries of the jet entrance were so designed to avoid such bifurcations of liquid jet. Diameter of the jet was measured at sufficiently downstream to avoid any error due to initial contraction or curvature of the surface of the jet at low velocity due to the presence of obstruction. As the ratio of the tube exit diameter to the diameter of solid rod were approximately 2.3 to 3, when only single rod was placed as the obstruction at the jet entrance it shows quiet different observations than that with two rods placed parallel to each other as shown in schematic diagram of the geometry of the jet entrance (Fig. 2). Placing two rods in such relatively narrow diameter opening causes the jet to reduce the overall area of opening suddenly on the upstream side and the columns of liquid passes from the opening area available between the rod and curved inside surface of

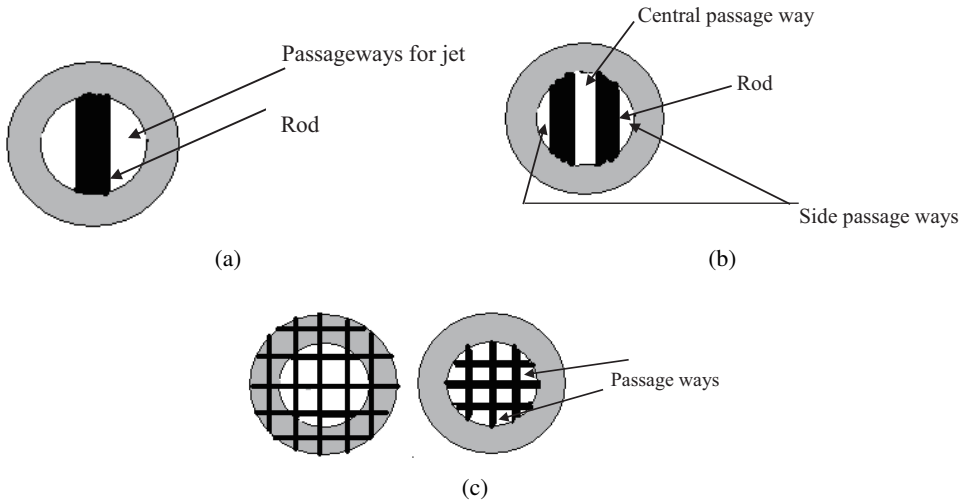


Figure 2: Geometries of the jet entrance (a) Solid rod placed at the centre of the jet entrance, (b) Two solid rods placed equidistant from the centre of the jet entrance, (c) Wire screen attached with the jet entrance

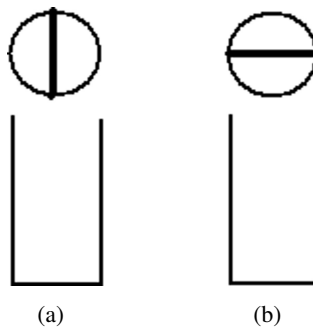


Figure 3: Locations of camera for jet facing, (a) direction parallel to axis of rod, (b) direction perpendicular axis of rod

the tube for side passage-ways (Fig. 2 (a, b)) get pushed towards central gateway where they collide with the central columnar jet and intermingle with each other as soon as they cross the obstruction. Further increasing in the obstruction by providing 10 mesh screen at the jet entrance by both ways as shown in Fig. 2 (c), caused the jet to become quiescent and at the downstream, the jet did not exhibit any expansion after initial contraction as shown in Fig. 4.

Splashing of jet is the general phenomena observed when it impinges on the substrate. If the *restriction* or *obstruction* is placed at some distance from the jet exit,

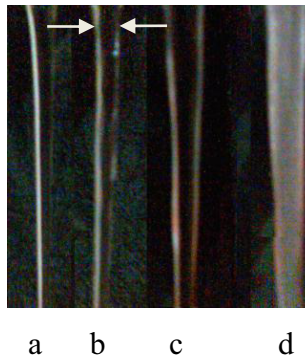


Figure 4: Images of jets with variety of obstructions at the entrance, the distance between arrows shows the boundary of the columnar jet, arrows show the jet diameter: (a) without rod, (b) single rod at the centre, (c) two rods at equidistance from centre, (d) with screen

the jet splashes and spreads in the direction so as to conserve the momentum and mass. If the restriction is designed to give separation of the continuous jet into branching, the purpose of the spreading of jet may be solved definitely but at the same time this results in high energy loss due to direct impingement and ultimate breakup length will suffer due to this phenomenon.

Providing a single rod at the centre of the jet entrance offered interesting results showing variation in the jet width measured from the direction perpendicular to the axis of the rod and that from parallel to the axis of the rod which is a common phenomenon generally observed at very low velocity jet from non-circular openings. The maximum diameter (or more appropriately, the width) of the jet was measured for the jet portion which has been completely stabilized for disturbances and at the same time jet remain in completely columnar shape. Jet velocities were measured from the calculation of average jet velocity at the jet entrance compensating the area of rod to have actual flow area available for flow.

Figure 5 presents better representation of variation of maximum jet width measured from the direction parallel to the axis of the rod with respect to jet velocity at tube exit. As the concentration of the glycerol increases, maximum jet width decreases. The difference in the maximum jet width attainable for different concentration of glycerol diminishes as the velocity increases. Furthermore, the deviation of the maximum width from the jet entrance opening diameter reduces with increasing viscosity and exit velocity of the jet.

As the viscosity increases, the maximum width of the jet, measured from direction perpendicular to the axis of the rod increases and approaches to the jet entrance

opening diameter for low exit velocity during starting of jetting period. At the same time, the maximum width of the jet measured from parallel direction to the axis of the rod show more deviation from the jet entrance opening diameter for any particular velocity and this deviation decreases as the velocity increases. Observation of the jet from the perpendicular direction to the axis of the rod shows such dynamics which are the characteristics of predominant viscous forces and momentum forces up to some extent in addition to surface tension, which cause the jet to propagate with gradual contraction in width as projected from the direction perpendicular to the direction of axis of the rod. As viscosity increases, the disturbed jet tries to attain the width same as that of the rod in the direction perpendicular to the axis of rod. And this dynamics is counter balanced by the momentum flux of the jet and surface tension as shown in Fig. 6 at low velocity the jet maximum diameter remains same as that of the rod length.

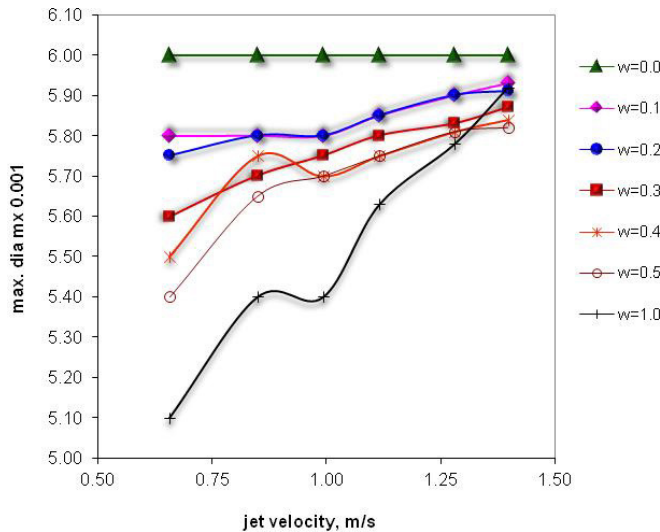


Figure 5: Maximum diameter from the direction parallel to the axis of the rod,  $w$  = mass fraction of glycerol in water

The jet exhibits little contraction at low velocity, and the maximum diameter of the jet gradually increases with the jet exit velocity when it observed from the direction parallel to the axis of the rod (see Fig. 7). Maximum jet diameter ratio is calculated by measuring maximum width of the jet in the atmospheric air and dividing it by the internal diameter of the tube from which the jet produces. At low concentration of glycerol, curve shows general behavior with is having some direct relationship with concentration of glycerol. As concentration increases, the jet shows some

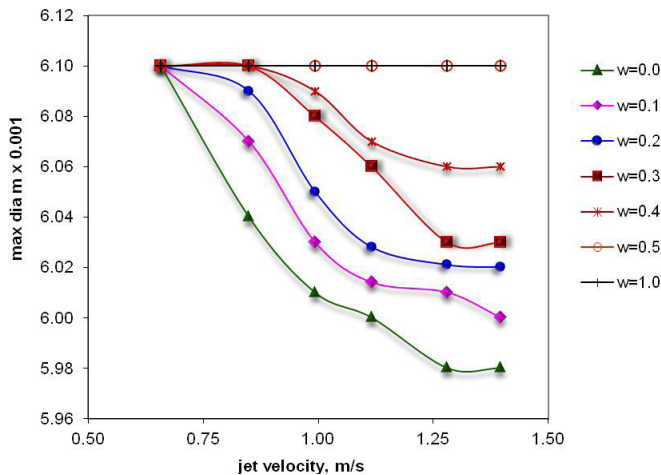


Figure 6: Maximum diameter from the direction perpendicular to the axis of the rod,  $w$  = mass fraction of glycerol in water

local peak at particular velocity and follows the trend afterwards. The trends shown in the Fig. 8 by jets of 40% and 100% glycerol necessitate careful attention on the geometry from right angle. It is necessary to know what happens with the geometry of the jet due to such type of obstructions and why it gives such surprising results.

Turning the facing direction of high speed camera, when we observed the jet from the direction perpendicular to the axis of solid rod, the diameter ratio found close to unity for low jet velocities and as velocity increases, the jet maximum diameter reduces gradually. Such reduction of the jet diameter is increases with reducing the concentration of glycerol. Similarly, as the concentration of the glycerol, and thus increasing the viscosity of the solution increases the maximum jet diameter and it remains almost constant for higher concentration jet as shown in Fig. 8 by the jets of 50% and 100% glycerol. Figures 7 and 8 suggest that the geometry of the jet get altered due to the presence of the obstruction at the jet entrance and more emphasizing is that it is not symmetric. Furthermore, Figs. 7 and 8 can not be used directly for making any judgment for relationship of viscosity and jet diameter or velocity and jet diameter as we have not accounted for surface tension change with concentration of glycerol and that is the reason why plots are given directly based on concentration and neither with respect to viscosity nor surface tension. These can be better understood plotting the geometry of the jet diameter against Weber number ( $We$ ) which is the measure of the ratio of inertial force to surface tension force, defined as [Dumouchel (2008); Dumouchel, Cousin, and Triballier (2005); Mayer and Branam (2004)]  $We = \rho u^2 d / \sigma$  where,  $\rho$  is the density,  $u$  is the relative

velocity,  $d$  is the diameter of jet, and  $\sigma$  is the surface tension.

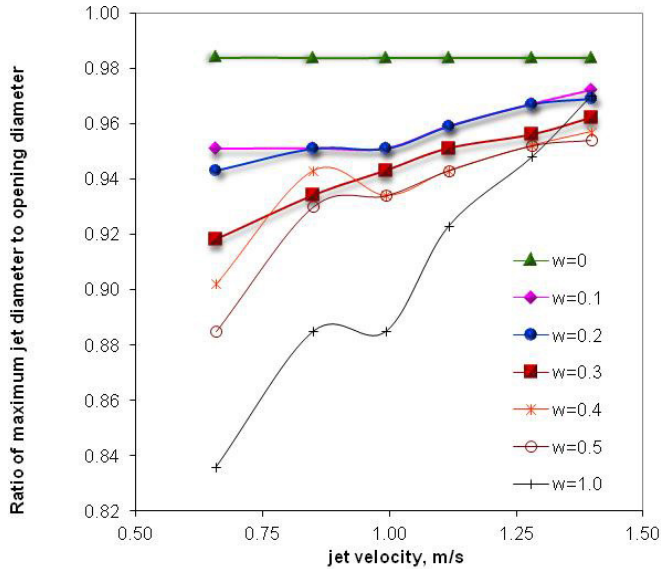


Figure 7: Maximum jet diameter ratio measured from direction parallel to axis of rod,  $w$  = mass fraction of glycerol in water

Figure 9 shows change in the *characteristic jet diameter ratio* – ratio of the maximum diameter more correctly the ratio of width of the jet measured from perpendicular direction to the width of the jet at the same cross section to parallel direction to the axis of rod for different concentrations of aqueous glycerol. The systematic calculation of such type of deformation induced due to the presence of obstruction at the nozzle exit may be of help to determine the dynamic surface tension as explained by oscillating jet technique by Howell, Megaridis, and McNallan (2004) in conjunction with the model developed by Bechtel, Cooper, Forest, Petersson, Reichard, Saleh, and Venkataraman (1995).

At a fixed Weber number, the *characteristic jet diameter ratio* - ratio of maximum width of jet measured perpendicular to the axis of bar to that of measured parallel to axis of bar - increases with decreasing concentration of glycerol in water, which means that the flow of jet becomes more symmetric as concentration of glycerol reduces in water. For water the ratio remains constant for the entire range of Weber number encountered in our experiments. Increase in Weber number cause the jet to become more symmetric and eventually the geometry of the jets will have almost similar orientation as it can be shown by the curves of characteristic diameter ratio as they tend to merge at higher Weber numbers. Ultimately the jet attains circular

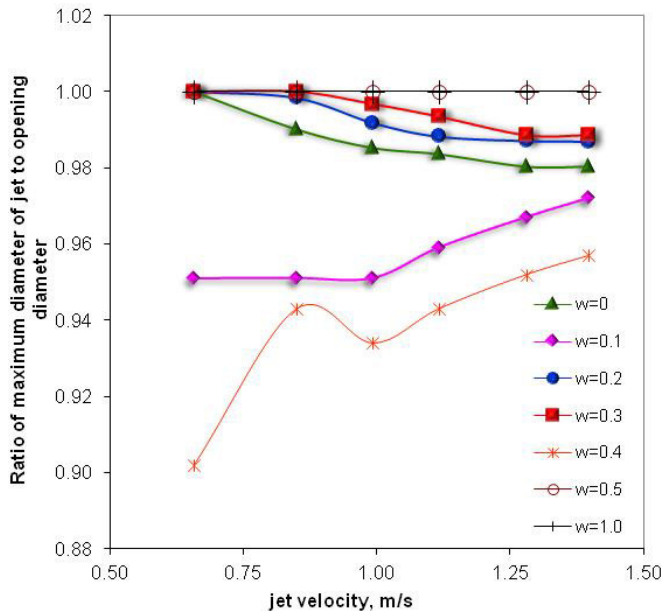


Figure 8: Maximum jet diameter ratio measured from direction perpendicular to axis of rod,  $w$  = mass fraction of glycerol in water

cross section due to the surface tension, but as the deformation of the columnar shape was the concern in the present study, the observations have been made in the vicinity of the jet entrance.

Figure 10 shows how the characteristic jet diameter ratio changes with Weber number. Trends of dynamics of jets of aqueous solutions of glycerol show certain dependency on Weber number. This was found calculating the power of the Weber number term which directly reflect the symmetry of the aqueous glycerol jet. It has been found that under experimental condition, as shown in Fig. 10, the maximum jet characteristic diameter ratio depends on concentration of glycerol as well as Weber number and the maximum characteristic jet diameter ratio observed at  $We^{(0.092 \cdot \text{mass fraction of glycerol})}$ .

### Hysteresis

Quite surprising phenomena were observed at certain higher velocity after the jet becomes turbulent as they shown expansion just after the exit of jet. As all the aqueous solutions exhibited such hysteresis at particular velocity, further increase in velocity again caused the jets to propagate more vigorously disappearing the maximum diameter, except the higher concentration of glycerol solutions, and polymeric

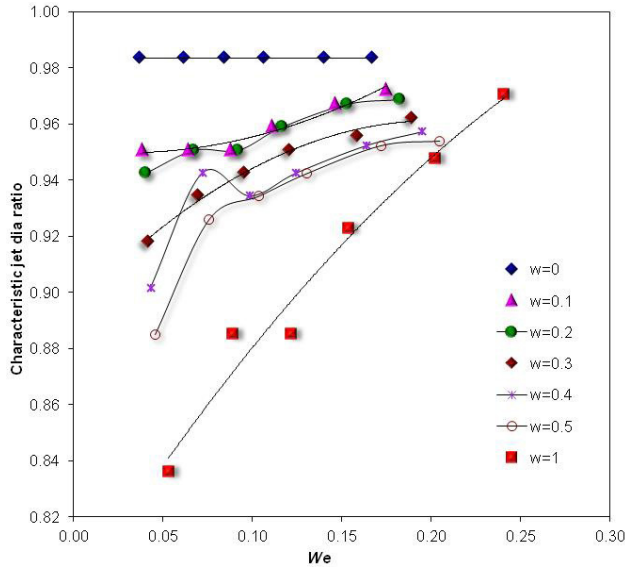


Figure 9: Characteristic jet diameter ratio at various Weber numbers,  $w$  = mass fraction concentration of glycerol in water

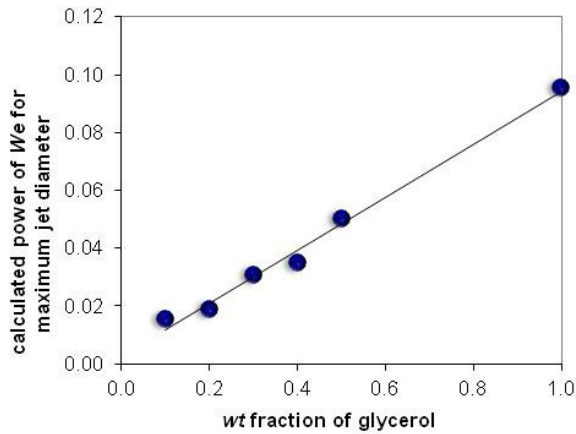


Figure 10: Maximum jet characteristic diameter ratio dependency on Weber number and mass fraction of glycerol in water

solution. As shown in Fig. 11, the expansion ratio decreased which is due to the increase of viscosity as the concentration of glycerol was increased.

The glycerol solutions more than 50% concentration did not show this phenomena,

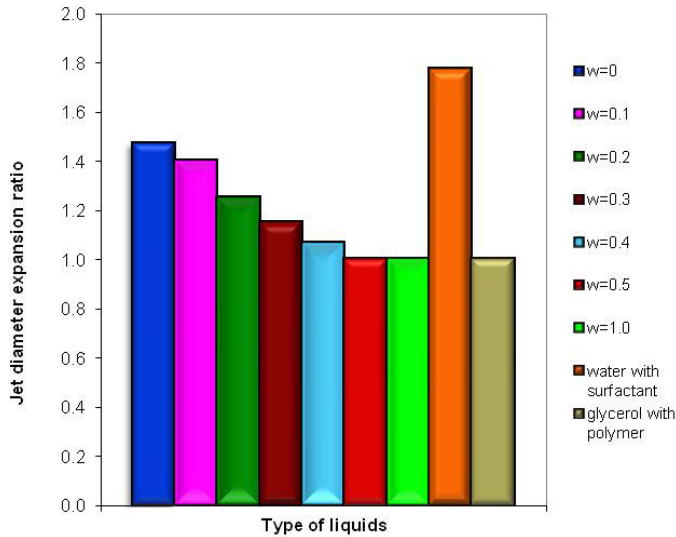


Figure 11: Jet diameter expansion ratio measured parallel to rod axis

and the jets did not fragmented but they exhibited surface perturbations. Similarly, addition of polyethylene oxide (1% by *wt*) also diminished any expansion of the jets of aqueous glycerol solutions while the addition of sodium lauryl sulphate in water (1.2% by *wt*) caused the jet to show more expansion approximately 80% than that of jet entrance diameter. We interpret these observations as the effect of polymer and surfactant on the dynamics of aqueous jets. Rigorous studies have been done on dynamics of liquid jet [McGough and Basaran (2006); Timmermans and Lister (2002); Uddin, Decent, and Simmons (2008); Xue, Corvalan, Dravid, and Sojka (2008); Young, Booty, Siegel, and Li (2009)], and film flow [Blyth and Pozrikidis (2004); Gao and Lu (2007)] to explore the effects of surfactants and polymers [Carroll and Joo (2009); Clasen, Bico, Entov, and McKinley (2009); Hoyt, Taylor, and Runge (1974); Mun, Byars, and Boger (1998); Roy, Morozov, van Saarloos, and Larson (2006)]. The fact is now well-known that the addition of drag reducing polymers in liquids elongates the jet breakup length. It is also now well understood that the addition of surfactants decreases surface tension in case of free liquid jet or interfacial tension in case of confined jet and lead to accelerated growth rate of perturbations and the reduces the jet breakup length. The addition of polymer causes the jet to be in more columnar shape. Due to long chain type of structure of polymeric molecules, the jet containing polymers does not show appreciable surface perturbations. Addition of sodium lauryl sulphate reduces the surface tension of solution which results in more separation of liquid threads and exhibits high jet

diameter expansion ratio. All these phenomena were observed for variable velocity ranges from 2.4 m/s for surfactant solution to 4 m/s with polymeric solutions.

#### **4 Conclusions**

The dynamics of aqueous glycerol jets have been studied to identify uneven jet expansion/contraction phenomena due to presence of an obstruction at the tube exit.

Images of the jets coming through such restricted entrance were captured by high speed camera from two locations, viz. keeping the camera parallel to the axis of the rod, and perpendicular to the axis of the rod. Due to the presence of the solid rod at the tube exit, the jet displayed surprising geometrical shapes. Its cross section became elliptical, with this effect being dependent on the concentration of glycerol or more precisely, on liquid properties such as surface tension and viscosity.

This led us to conceive the idea that measuring the characteristic diameter ratio of the jet at a particular down stream location could be used to determine indirectly the surface tension and viscosity of the considered liquid. Therefore, a new direction of research could be initiated for the design of new instruments for the measurement of such properties based on the measurement of the controlled deformation attained by liquid jets with known obstruction geometry.

**Acknowledgement:** The authors acknowledge S. V. National Institute of Technology, Surat-395007, Gujarat, India, for the support through Research and Development Project.

#### **References**

**Bechtel, S.; Cooper, J.; Forest, M.; Petersson, N.; Reichard, D.; Saleh, A.; Venkataramanan, V.** (1995): A new model to determine dynamic surface tension and elongational viscosity using oscillating jet measurements. *Journal of Fluid Mechanics*, vol. 293, pp. 379–403.

**Begenir, A.; Tafreshi, H. V.; Pourdeyhimi, B.** (2004): Effect of nozzle geometry on hydroentangling water jets: Experimental observations. *Textile Research Journal*, vol. 74, no. 2, pp. 178–184.

**Bird, R. B.** (2002): Transport phenomena. *Applied Mechanics Reviews*, vol. 55, no. 1, pp. R1–R4.

**Blyth, M.; Pozrikidis, C.** (2004): Effect of surfactant on the stability of film flow down an inclined plane. *Journal of Fluid Mechanics*, vol. 521, pp. 241–250.

**Carroll, C. P.; Joo, Y. L.** (2009): Axisymmetric instabilities in electrospinning of highly conducting, viscoelastic polymer solutions. *Physics of Fluids (1994-present)*, vol. 21, no. 10, pp. 103101.

**Clasen, C.; Bico, J.; Entov, V.; McKinley, G.** (2009): ‘gobbling drops’: the jetting–dripping transition in flows of polymer solutions. *Journal of fluid mechanics*, vol. 636, pp. 5–40.

**Craster, R.; Matar, O.; Papageorgiou, D.** (2009): Breakup of surfactant-laden jets above the critical micelle concentration. *Journal of Fluid Mechanics*, vol. 629, pp. 195–219.

**Dumouchel, C.** (2008): On the experimental investigation on primary atomization of liquid streams. *Experiments in fluids*, vol. 45, no. 3, pp. 371–422.

**Dumouchel, C.; Cousin, J.; Triballier, K.** (2005): On the role of the liquid flow characteristics on low-weber-number atomization processes. *Experiments in fluids*, vol. 38, no. 5, pp. 637–647.

**Gao, P.; Lu, X.-Y.** (2007): Effect of surfactants on the inertialess instability of a two-layer film flow. *Journal of Fluid Mechanics*, vol. 591, pp. 495–507.

**Hiroyasu, H.** (2000): Spray breakup mechanism from the hole-type nozzle and its applications. *Atomization and Sprays*, vol. 10, no. 3-5.

**Howell, E.; Megaridis, C.; McNallan, M.** (2004): Dynamic surface tension measurements of molten sn/pb solder using oscillating slender elliptical jets. *International journal of heat and fluid flow*, vol. 25, no. 1, pp. 91–102.

**Hoyt, J.; Taylor, J.; Runge, C. D.** (1974): The structure of jets of water and polymer solution in air. *Journal of Fluid Mechanics*, vol. 63, no. 04, pp. 635–640.

**Kanemura, T.; Yoshihashi-Suzuki, S.; Kondo, H.; Sugiura, H.; Yamaoka, N.; Ida, M.; Nakamura, H.; Matsushita, I.; Muroga, T.; Horiike, H.** (2011): Characteristics of free-surface wave on high-speed liquid lithium jet for ifmif. *Journal of Nuclear Materials*, vol. 417, no. 1, pp. 1303–1306.

**Lee, K.; Aalburg, C.; Diez, F. J.; Faeth, G. M.; Sallam, K. A.** (2007): Primary breakup of turbulent round liquid jets in uniform crossflows. *AIAA journal*, vol. 45, no. 8, pp. 1907–1916.

**Mayer, W.; Branam, R.** (2004): Atomization characteristics on the surface of a round liquid jet. *Experiments in fluids*, vol. 36, no. 4, pp. 528–539.

**McGough, P. T.; Basaran, O. A.** (2006): Repeated formation of fluid threads in breakup of a surfactant-covered jet. *Physical review letters*, vol. 96, no. 5, pp. 054502.

**Mun, R. P.; Byars, J. A.; Boger, D. V.** (1998): The effects of polymer concentration and molecular weight on the breakup of laminar capillary jets. *Journal of Non-Newtonian Fluid Mechanics*, vol. 74, no. 1, pp. 285–297.

**Roy, A.; Morozov, A.; van Saarloos, W.; Larson, R. G.** (2006): Mechanism of polymer drag reduction using a low-dimensional model. *Physical review letters*, vol. 97, no. 23, pp. 234501.

**Timmermans, M.-L. E.; Lister, J. R.** (2002): The effect of surfactant on the stability of a liquid thread. *Journal of Fluid Mechanics*, vol. 459, pp. 289–306.

**Uddin, J.; Decent, S.; Simmons, M.** (2008): The effect of surfactants on the instability of a rotating liquid jet. *Fluid dynamics research*, vol. 40, no. 11, pp. 827–851.

**Wu, P.-K.; Miranda, R.; Faeth, G.** (1995): Effects of initial flow conditions on primary breakup of nonturbulent and turbulent round liquid jets. *Atomization and Sprays*, vol. 5, no. 2.

**Xue, Z.; Corvalan, C. M.; Dravid, V.; Sojka, P. E.** (2008): Breakup of shear-thinning liquid jets with surfactants. *Chemical Engineering Science*, vol. 63, no. 7, pp. 1842–1849.

**Young, Y.-N.; Booty, M.; Siegel, M.; Li, J.** (2009): Influence of surfactant solubility on the deformation and breakup of a bubble or capillary jet in a viscous fluid. *Physics of Fluids (1994-present)*, vol. 21, no. 7, pp. 072105.

